

# **THE USE OF HORIZON CAMERA, DOPPLER NAVIGATOR, AND STATOSCOPE IN AERIAL TRIANGULATION**

by Dr. J. M. ZARZYCKI

Vice President, Canadian Aero Service Limited, Ottawa

---

(Paper presented to the 10th Congress of the International Society of Photogrammetry, Lisbon, 1964)

## **1. — INTRODUCTION**

The extension of control by photogrammetric methods in unmapped territories is one of the most challenging tasks of photogrammetric engineering. Many aerial triangulation methods have been developed, based either on the analogue or the analytical approach to the problem. The ultimate aim is to devise a photogrammetric system which would permit compilation of maps from data collected by airborne instruments, thus effecting a very considerable reduction, if not complete elimination, of ground control surveys. The use of auxiliary instruments, such as the horizon camera, Doppler navigator, and statoscope, together with the aerial camera, is a step in this direction.

Aerial triangulation techniques, based on a successive orientation of one photograph to the next, are limited to a large degree by a double summation of accidental and systematic errors. This limitation exists when analogue instruments, such as the Wild A-7 and Zeiss C-8, are employed, as well as when stereo-comparators or mono-comparators and analytical methods are used.

The only hope of eliminating this unfavourable summation of errors lies in the introduction of additional data obtained from auxiliary instruments installed in the survey aircraft. One of the auxiliary instruments introduced again to photogrammetry is the horizon camera. The horizon camera is the only instrument commercially available that can provide tip and tilt information with a high degree of accuracy. It is simple in construction and operation, and is relatively inexpensive.

The Doppler navigator, developed originally for military purposes, was quickly adopted for civilian photogrammetric applications. It guides the

aircraft on a survey flight and triggers the aerial camera at predetermined intervals, thus determining the distance between each exposure station.

The statoscope gives the difference in elevation between exposure stations relative to an isobaric surface. This instrument has been used in aerial triangulation for some time. Introduction of these auxiliary data, particularly the tip and tilt derived from the horizon camera, into the bridging procedure eliminates the double summation of errors and, consequently, cancels the need for vertical control in the center of the strip.

Canadian Aero Service Limited has successfully employed the horizon camera, Doppler navigator, and statoscope on projects in Nigeria involving mapping at 1/50 000 with 50-foot (15.5-metre) contours of some 100 000 km<sup>2</sup>, on a project in Gabon involving mapping at 1/5 000 with 10-metre contours for a 1 000-km long railway, and on a project in northern Canada involving extension of control in an area of some 11 000 km<sup>2</sup> for mapping at 1/50 000 with 25-foot (7.8-metre) contours.

The horizon camera is presently being used on an Aerodist survey project in Canada as an integral part of a mapping system which permits an accurate determination of  $x$ ,  $y$ , and  $z$  coordinates of the nadir point of each vertical aerial photograph. The tip and tilt of each photograph at the moment of exposure, determined from the horizon camera, is used for location of the nadir point of each Aerodist-controlled vertical photograph.

To date we have processed close to 5 000 horizon photographs and successfully carried out aerial triangulation. We utilized the tip and tilt information derived from the horizon camera in addition to data provided by Doppler navigator and statoscope. This practical experience yielded a large amount of data for a critical evaluation of the mapping system.

This paper will discuss this mapping system, the methods employed in aerial triangulation, and the results achieved.

## 2. — HORIZON CAMERA

### 2.1 — General Description

The function of the horizon camera is to determine the relative tip and tilt of each aerial photograph at the moment of exposure.

The first horizon camera was developed in Finland by NENONEN in 1928 and was manufactured by Zeiss Aerotopograph Company. It photographed the horizon in two perpendicular directions. The results obtained in experimental working using this horizon camera, by von GRUBER, SCHERMERHORN, NEUMAIER, BRUHLACHER, LÖFSTRÖM, and HALONEN, as well as the results achieved in practical applications in Finland, indicated great possibilities for the use of this auxiliary instrument in photogrammetric mapping. Unfortunately, the horizon camera did not find much application outside of Finland and was almost forgotten by the end of the Second World War.

In 1960, a new horizon camera, designed by LÖFSTRÖM and built by the Wild Company, became available. This camera photographs, by means of four separate objectives, the horizon in four directions (forward, aft, left, and right) on a 35-mm film. An adjustable counter and a seconds clock are also photographed on the same negative. The focal length of each of the four objectives is approximately 32 mm; lens aperture  $f/5.6$ ; viewing angle  $39^\circ$ . There is no provision for changes of the lens aperture, or of the exposure time.

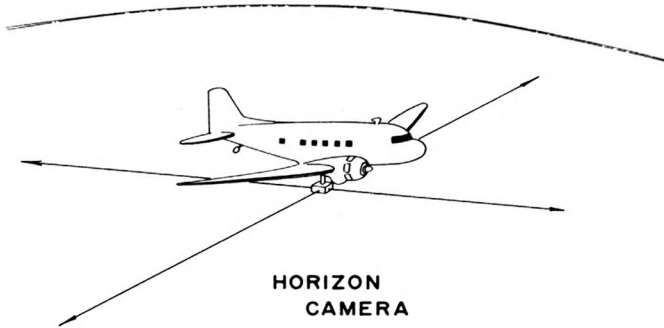
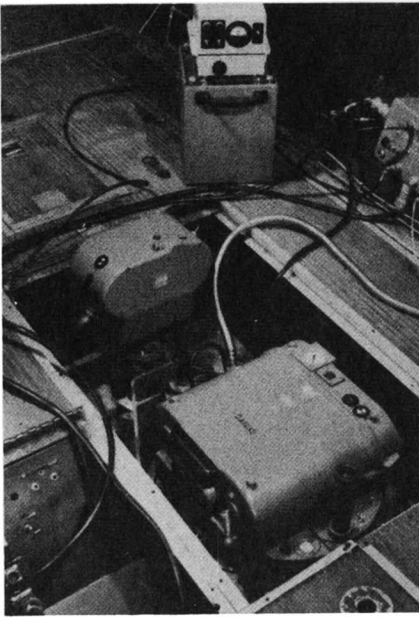
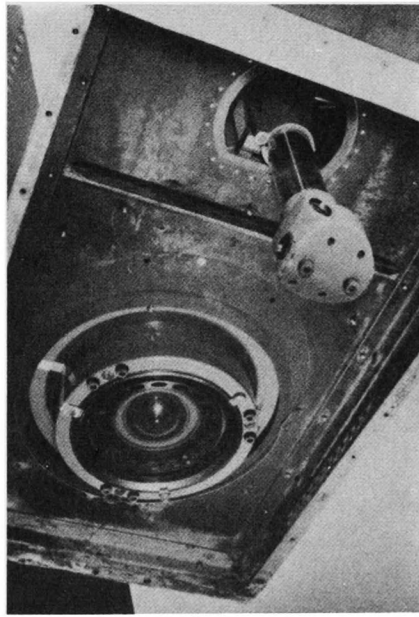


FIG. 1. — Principle of the horizon camera.

The prototype of the horizon camera was equipped with three fiducial marks along the center line for each of the four horizon pictures. On the recommendation of the author, two fiducials were added in the latest models of the horizon camera. This allows the horizon to be measured in five



2



2a

FIG. 2. — Installation of the Wild RC-9 aerial camera, Wild horizon camera, and Zeiss statoscope in a DC-3 aircraft.

FIG. 2a. — Outside view of the RC-9 and horizon camera installation in a DC-3 aircraft.

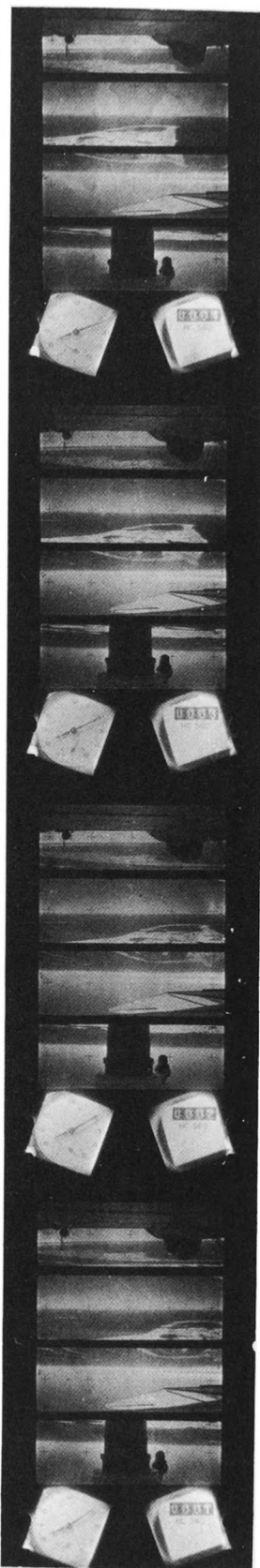


FIG. 3. — Typical horizon photographs.

locations. It also makes it possible to use the horizon pictures when one of the outside fiducials is obscured by portions of the aircraft radio or Aerodist antennas.

The horizon camera rests in the same mount as the vertical aerial camera. Consequently both cameras are tipped and tilted simultaneously and by the same amount. A universal servo mount PAU-2 holds either an RC-8 or RC-9 camera in addition to the horizon camera. A connecting rod between the vertical camera and the horizon camera is provided for simultaneous drift adjustment.

The horizon photographs are synchronized with the vertical photographs in two ways :

- (a) by zeroing exposure counters on both the RC-9 and the horizon camera before each flight. Both counters are operated by the same electrical impulse, and the same exposure number appears on both negatives ( $9 \times 9$  inches and 35-mm);
- (b) by recording the time on both negatives at the moment of exposure. The clocks on the vertical camera and on the horizon camera are synchronized before each flight.

## 2.2 — Technique of Obtaining Horizon Photographs

To obtain acceptable horizon photographs under variable atmospheric conditions, much attention must be paid to the choice of proper emulsions and filters. The horizon that appears on the negatives is not a true horizon but a vapour horizon, or a very distant cloud layer. Pictures of the true horizon can be obtained only over water or under certain atmospheric conditions, when flying at low altitudes. However, it is not important whether the true horizon or a vapour horizon be photographed since we are determining the values of relative tip and tilt. It is important that the horizon appear on the negatives as a sharp, well-defined line that can be

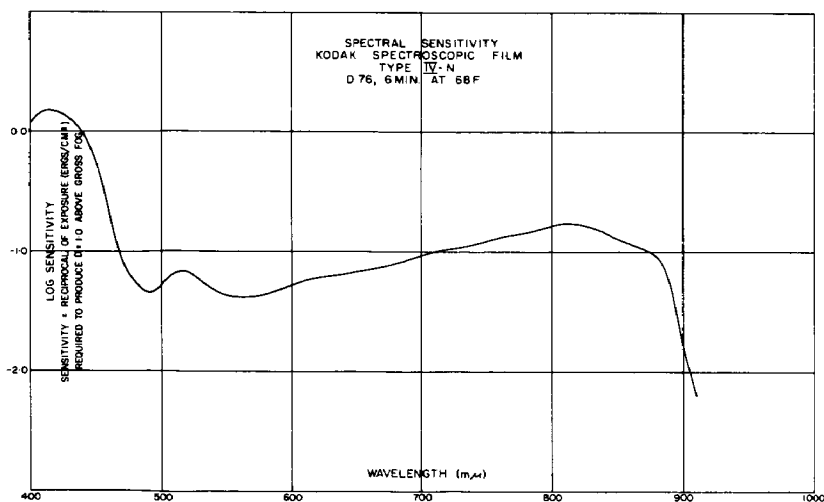


FIG. 4. — Spectral sensitivity of film presently used for horizon photography.

measured under magnification. Therefore, the film for horizon pictures must yield maximum contrast and be of fine grain.

In Nigeria and in Canada we used the Kodak High Speed Infra-red Film. This film is of medium-class contrast, resolution of 69 to 95 lines/mm, and of medium grain. To control exposure time, neutral density filters were used in addition to infra-red filters. This film provided acceptable horizon photographs. Later, after considerable experimentation, we selected a new type of film, the Kodak Spectroscopic Film, type 4N. This film is of very high contrast, very high resolution (136 to 225 lines/mm), and of fine grain. Spectral sensitivity of this film is shown on Fig. 4. Using this film in Canada and Nigeria, high-quality horizon photos were obtained under average atmospheric conditions, and photos of acceptable quality under marginal weather conditions.

### 2.3 — Measurement of the Horizon Photographs

Let us assume that Figures 5 and 5a represent the horizon lines corresponding to the vertical photographs  $i$  and  $i + 1$  respectively. Let us assume further that horizon photographs  $i$  and  $i + 1$  were taken in the direction of flight. The difference in the position of the horizon line in photos  $i$  and  $i + 1$ , relative to their fiducial marks, is proportional to the difference in tip of the corresponding vertical photographs. If we place these horizon photos under a stereoscope, so that the corresponding fiducial marks in both photos overlap in the optical model, we can observe the horizon in three dimensions. The fiducial marks will form a reference plane and the horizon line will appear in three dimensions: either above, below, or intersecting the reference plane. This stereo effect is caused by the displacement of the horizon line in photo  $i + 1$  relative to photo  $i$ . This displacement or parallax is measured using a Wild stereo-microscope, and the relative tip and tilt are computed.

A reference horizon photo is placed in the left frame of the stereo-microscope so that the horizon line is approximately perpendicular to the

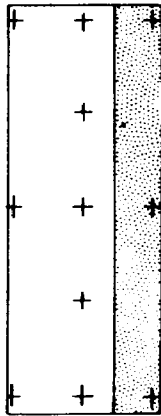


FIG. 5

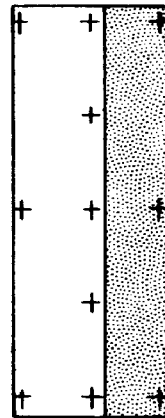


FIG. 5a

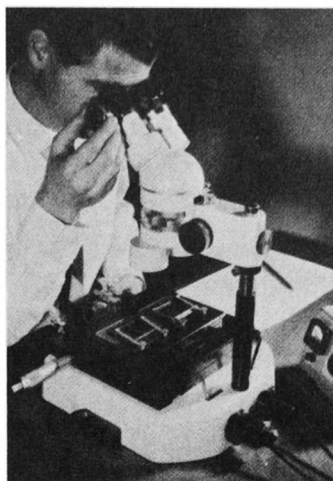


FIG. 6. — Wild stereomicroscope used for measuring horizon photographs.

instrument base. The other horizon photos of the same strip are placed one by one in the right frame in the same position.

The horizontal parallaxes of the central fiducial marks (crosses  $R_1, R_2, R_3, R_4, R_5$ ) and the horizontal parallaxes of the adjacent points on the horizon line ( $h_1, h_2, h_3, h_4, h_5$ ) in corresponding horizon photos are stereoscopically measured using the floating mark (Fig. 7). The differences of these parallax readings,  $R_1 - h_1, R_2 - h_2, R_3 - h_3, R_4 - h_4, R_5 - h_5$ , express the displacement of the horizon line in the measured horizon photo relative to the horizon line in the corresponding reference horizon photo. The expression

$$\frac{(R_1 - h_1) + (R_2 - h_2) + (R_3 - h_3) + (R_4 - h_4) + (R_5 - h_5)}{5}$$

is the vertical displacement of the horizon line of the measured photo relative to the corresponding reference horizon photo.

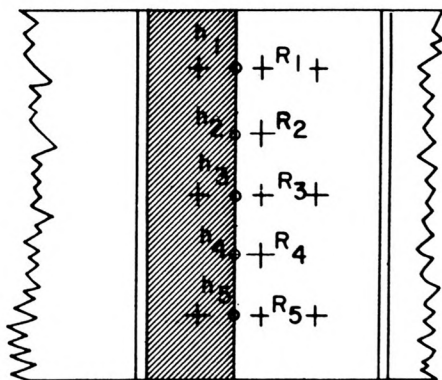


FIG. 7

The equation,

$$\alpha = \frac{(R_1 - h_1) + (R_2 - h_2) + (R_3 - h_3) + (R_4 - h_4) + (R_5 - h_5)}{5} \cdot \frac{\rho^c (*)}{f} \quad (1)$$

(\*)  $\rho^c$  is the value of one radian expressed in centesimal minutes.

In the rest of the text, symbol  $c$  indicates that the quantity is expressed in centesimal minutes.

where  $f$  is the focal distance of the horizon camera, gives the relative difference in inclination ( $\Delta\varphi$ ,  $\Delta\omega$ ) of the aerial camera between the measured photo and the reference photo.

Since horizon photos are taken in four perpendicular directions, the tip and tilt can be determined twice: the tip ( $\varphi$ ) from the forward and the aft photos; and the tilt ( $\omega$ ), from the left and the right photos.

The differential tip and tilt can also be determined in a different manner from the differential inclination of the horizon line. In this case, the left or the right photo is used for the determination of  $\varphi$ , and the forward or aft photo for the determination of  $\omega$ .

The equation

$$\beta = [(R_1 - h_1) - (R_5 - h_5)] \cdot \frac{\rho^{\circ}}{d} \quad (2)$$

expresses the difference in the inclination of the horizon line between the reference photos and the measured photos. In equation (2),  $d$  is the distance between fiducials  $R_1$  and  $R_5$ , and equals approximately 22 mm.

To investigate the accuracy of computing tip and tilt by means of equations (1) and (2), let us assume that the standard error of one parallax observation is  $m_p$ . Applying the formulae from the theory of errors to equations (1) and (2), we get the standard errors of tip and tilt as follows:

(a) using equation (1)

$$m_{\alpha^{\circ}} = \pm 128 m_p$$

(b) using equation (2)

$$m_{\beta^{\circ}} = \pm 582 m_p$$

where  $m_p$  is expressed in mm.

From the above, it is evident that the determination of tip and tilt by equation (1) is more accurate. Therefore, we are using it in our computations.

If all the four horizon photos are available, the averages of the results obtained from the forward and aft, and from the left and right photos are taken as the final values of  $\varphi$  and  $\omega$  respectively. The differential tips and tilts are measured between a reference photo and each consecutive photo of a flight line, in the manner illustrated in the figure below:

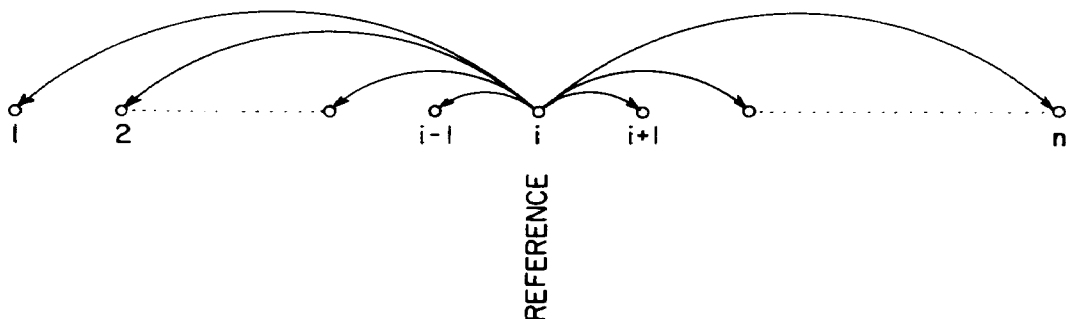


FIG. 8



The above method of measurement provides independent values of tip and tilt for each vertical photograph. Consequently, summation of errors in  $\varphi$  and  $\omega$  is eliminated.

As the forward and aft horizon photographs record the same segment of their respective horizons when on the same flight line, it is possible to choose a reference picture for the determination of  $\varphi$  at intervals of 20 to 25 pictures. For the determination of  $\omega$ , it is advisable to choose reference pictures at 8- to 10-picture intervals because the viewing angle of the camera is only  $39^\circ$ . We have successfully measured differential tip and tilt ( $\Delta\varphi$  and  $\Delta\omega$ ) using photographs of different flight lines flown on the same day.

The determination of the differential tip and tilt for horizon photos of an average quality can be repeated with a precision of  $\pm 1^\circ$ .

#### 2.4 — Determination of Absolute $\varphi$ and $\omega$

To determine the absolute values for tip and tilt, it is desirable that at least one stereo model in each flight line be leveled on ground control points or on water bodies. The minimum ground control requirement is that at least one stereo model in a group of flight lines flown on the same day be fully controlled in elevation. After this stereo model is carefully leveled, the tip and tilt of each photograph making up this stereo model is determined in the plotting instrument.

The absolute values of tip and tilt for each successive photograph are determined by adding to the absolute  $\varphi$  and  $\omega$  of the controlled photograph, the differences in  $\varphi$  and  $\omega$  computed from horizon photos for each vertical photograph of a flight line. In order to check the determination of the absolute tip and tilt, we also provide vertical control for the last stereo model of each flight line. The results are considered to be correct if a closure is obtained with an accuracy equivalent to that of the relative orientation, usually  $\pm 2^\circ$  to  $\pm 3^\circ$ .

The values of  $\varphi$  and  $\omega$  determined by the above described methods must be corrected for the influence of earth curvature before they can be used in a plotting instrument.

Let us assume that photographs 1 and 2 were exactly vertical, that is, with the tip and tilt of each equal to zero, ( $\varphi_1 = 0$ ,  $\omega_1 = 0$ ,  $\varphi_2 = 0$ ,  $\omega_2 = 0$ ). While the camera axes of these photos will be normal (vertical) to the geoid in their respective locations, they will not be parallel. The convergence of these axes is equal to the angle  $\gamma$  which is proportional to the distance between the pictures and the radius of the earth. To achieve a parallax-free model, the relations of the camera axes have to be reproduced in the plotting instrument, that is, they must have the same convergence angle  $\gamma$ . Therefore, the values of  $\varphi$ , derived from the horizon photos, need to be corrected for this convergence before they can be introduced into the plotting instrument. When photo 1 is introduced into the left plate holder of the instrument, the value of  $\gamma/2$  has to be added to the  $\varphi_1$  derived from the horizon camera. When photo 2 is introduced into the right plate holder,

the value of  $\gamma/2$  has to be subtracted from the  $\varphi_2$  determined from the horizon camera for picture 2. Thus :

$$\begin{aligned}\varphi_1 \text{ (instrument)} &= \varphi_1 \text{ (horizon)} + \gamma/2 \\ \varphi_2 \text{ (instrument)} &= \varphi_2 \text{ (horizon)} - \gamma/2\end{aligned}$$

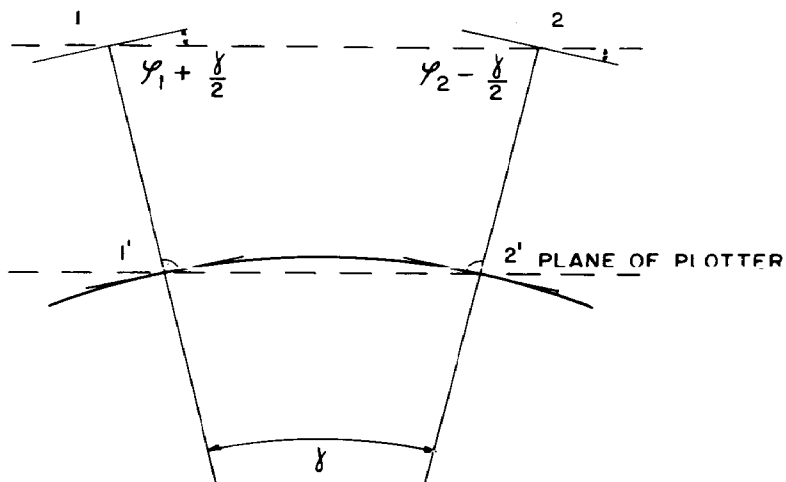


FIG. 9

### 3. — DOPPLER NAVIGATIONAL SYSTEM

The Doppler navigator, or navigational system, measures the ground speed and drift angle of an aircraft in flight. The system (Fig. 10) controls each flight in a predetermined direction, thus maintaining specified overlap between flight lines. It also triggers the aerial camera at predetermined distances and hence it establishes the forward overlap.

The Doppler navigational system is self-contained and does not require any ground stations. It demands only one assumption of basic information, that we know the starting point. Electronic waves transmitted from the aircraft to the ground are reflected and received again in the aircraft. Because of the relative motion of the aircraft to the ground, the frequency of the reflected signal differs slightly from the transmitted one. This difference in frequency is due to the Doppler effect.

The Radan-Doppler navigational system employed by us is manufactured by General Precision Laboratories of New York. A compact antenna-receiver-transmitter, mounted in the aircraft (Fig. 11), transmits four beams of pulsed microwave energy toward the earth : two at a time in diagonal pairs, with left-front, right-rear; then right-front, left-rear, by means of a specially designed slotted-planar-array antenna. Echoes of these signals, shifted in frequency by an amount proportional to the aircraft's ground speed, are received back in the plane.

The drift angle is found by comparing the Doppler frequency of one of the diagonal pairs with the Doppler frequency of the other diagonal

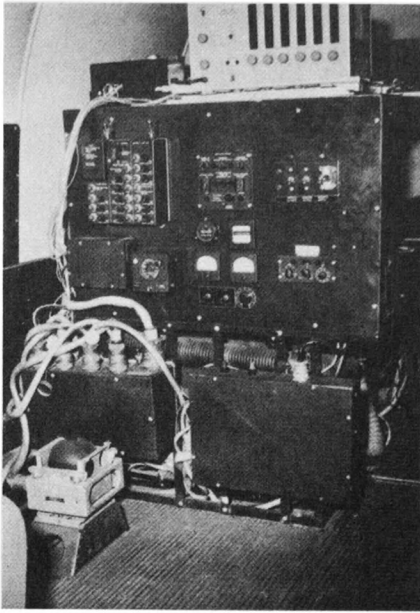
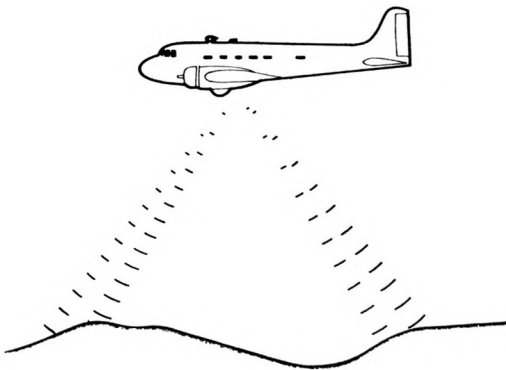


FIG. 10. — Installation of Doppler navigator in a DC-3 aircraft.

pair. The ground speed is found by measuring the beat frequency produced when reflected ground signals received by the forward-looking beam are mixed with those received by the backward-looking beam.

The system includes a course and distance computer, a Kearfott J-4 compass, and a specially designed computer to track the aircraft on a set course. It provides the aircraft's position continuously and does not require ground stations.

The data from the Doppler navigator is computed and visually presented to the pilot instantly. Before the Doppler unit is turned on at the beginning of the first flight line of each mission, two parameters, line length and magnetic azimuth, are set in the computer. It then begins to indicate deviations left or right of track and counts elapsed mileage on a visual



DOPPLER —

4 RADAR BEAMS

FIG. 11

indicator. During the flight of each line the parameters of the next line are introduced into a second circuit of the computer. These are line length, magnetic azimuth, and offset (line spacing).

### 3.A STATOSCOPE

The Wild or Zeiss statoscope registers the difference of each exposure station relative to an isobaric surface. The statoscope is not an absolutely necessary element of the mapping system when the horizon camera is used, but it constitutes a valuable addition in certain aerial triangulation techniques discussed later in this paper. The slope of the isobaric surface can be computed by the following formula :

$$\Delta h_{\text{feet}} = 0.035 v \cdot d \cdot \sin \alpha \cdot \sin \varphi \quad (3)$$

where

- $\varphi$  is the air speed in miles per hour
- $v$  = distance from the starting point
- $d$  is the drift angle, and
- $\alpha$  is the approximate latitude.

The Doppler navigator computer determines continuously the true air speed, the drift angle, and the distance along the track.

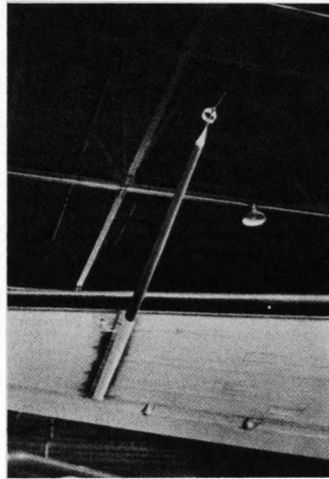


FIG. 12. — Installation of the static probe.

To provide an accurate source of static pressure for the statoscope, a special swivel probe was installed (Fig. 12) near the tip of the wing, approximately two chord lengths forward of the leading edge of the wing. The probe consists of a set of concentric cylinders expanding rearward, always with a diameter less than one-tenth the distance from the tip. Holes are drilled at right angles to the surface. The swivel probe is supported at the center of gravity and carries a ring behind the centroid so that it will weathercock and keep a constant attitude to the air flow.

The statoscope is connected to the static probe. We employed both the Wild and Zeiss Statoscope and the Litton Pressure Altimeter.

#### 4. — AERIAL TRIANGULATION TECHNIQUES

##### 4.1 — General

The auxiliary instruments described above provide the following orientation elements of the aerial camera at the moment of exposure :

- |                        |  |
|------------------------|--|
| Horizon Camera . . . . | determines $\varphi$ and $\gamma$ for each of the aerial photographs   |
| Doppler Navigator ..   | guides the aircraft on a predetermined course, determines distance between each exposure station, and yields data necessary for computation of the slope of the isobaric surface |
| Statoscope . . . . .   | determines the difference in elevation of each exposure station relative to an isobaric surface.   |

The most valuable for aerial triangulation is the horizon camera because it provides tip and tilt information with a high degree of accuracy. Introduction of the independent  $\varphi$  and  $\omega$  data in the aerial triangulation procedure eliminates the double summation of errors present in aerial triangulation without the use of such auxiliary data.

Integration of the data from these auxiliary instruments into a single mapping system suggests new approaches to the problem of extending control by photogrammetric methods. Independent stereo pairs of different flight lines can be combined into one block. It is possible to bridge entire areas rather than strips. This approach permits greater flexibility in the planning of flight lines, in the selection of the method of bridging, in the location of ground control, and in the choice of photogrammetric instruments for triangulation.

##### 4.2 — Instruments for Aerial Triangulation

The aerial triangulation methods based on the transferring of the elements of absolute orientation from one stereo model to the next by means of instrumental procedures or analytical methods necessitate the use of expensive first-order plotting instruments or comparators. When the orientation elements of the aerial camera are determined from auxiliary instruments, simple photogrammetric plotting instruments such as the Wild B-8 Autograph can be used for aerial triangulation. The important requirement such a plotter must fulfill is that it be stable and be equipped for accurate introduction of  $\varphi$  and  $\omega$  on the left and right plate holders. We have used the Wild B-8 very successfully for aerial triangulation in conjunction with vertical super-wide angle photography obtained with the Wild RC-9 camera.

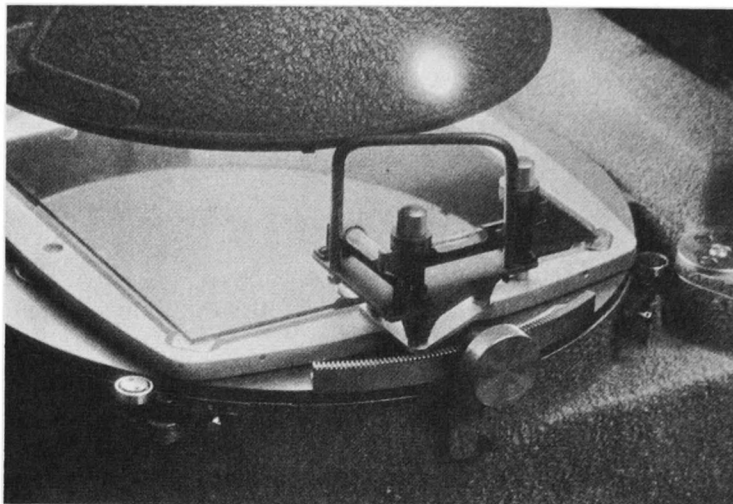


FIG. 13. — L-shaped level bubbles for registration of  $\varphi$  and  $\omega$  in the B-8 plotter.

The slight modifications which we made to the B-8 to permit accurate introduction of  $\varphi$  and  $\omega$  on the left and right plate holders are :

- (a) an extension to the plate holders to permit placing of precise L-shaped bubbles;
- (b) adding specially designed L-shaped bubbles to allow accurate introduction of tip and tilt in each camera (Fig. 13). Two 20-second bubbles were mounted on a stable platform in the shape of the letter L. The bubbles, when placed on the plate holder, are parallel to the  $x$  and  $y$  axes of the  $9 \times 9$  inch diapositives. Each bubble can be tilted in the vertical direction. Drums attached to the vertical screws permit direct readings of  $\varphi$  and  $\omega$  to an accuracy of  $1^c$  (30 seconds).

The B-8 is very carefully calibrated. Precise grid plates are used to determine the zero readings,  $\varphi_0$  and  $\omega_0$ , for both the left and the right plate holders and also to determine the zero value for general  $\Phi$ .

It is more convenient to use the level bubbles for the introduction of  $\varphi$  and  $\omega$  than the plotter's drums, because these drums show tip and tilt measured with reference to the fixed instrumental axes, whereas the horizon camera gives tip and tilt measured with reference to the axes of the aerial photograph. Orientation of these axes varies with the drift (swing) of the aerial camera at the moment of exposure. Since the level bubbles are located directly on the plate holders, they move or swing together with the diapositives and the data from the horizon camera can be introduced directly. If, however, the instrument drums are to be used, the horizon camera data must be corrected for the influence of swing.

#### 4.3 — Instrumental Procedure

##### 4.3.1 — *Using the B-8 or Other Instruments not having $b_z$ Movement*

The aerial triangulation is carried out by the independent pairs method, utilizing the data derived from the horizon camera and data given

by the Doppler unit. The absolute orientation of the stereo model can be determined either by introducing the  $\varphi$  and  $\omega$  on the left plate holder or on the right plate holder of the B-8 plotter. The absolute orientation of the model will differ, depending on which is used, because of errors in relative orientation and errors in the horizon camera readings.

The procedure finally adopted was this: the base distance given by Doppler navigator was introduced into the B-8 and the stereo model was oriented relatively; then the absolute value for  $\varphi$  and  $\omega$  was introduced in the B-8, first on the left and then on the right plate holders. The average values for  $\varphi$  and  $\omega$  for the left photograph and for the right photograph were computed from both these determinations and were introduced into the plotting instrument to establish the absolute orientation of the stereo model. This method of determining absolute orientation minimizes the effect of inaccuracies in the relative orientation on the absolute orientation of the stereo model. The vertical datum was not carried by the stereo operator. The elevations of each pass point were read on an arbitrary vertical datum, and the models were connected mathematically during adjustment. After the absolute orientation of the model was determined, the operator pricked pass points required for stereo templates on stable plastic material.

#### 4.3.2 — *Using Instruments Equipped with $b_x$ and $b_y$ Movements*

When the instrument used for aerial triangulation is provided with a  $b_x$  component, the procedure differs slightly. After introduction of the base distance given by Doppler navigator the  $y$ -parallax is removed with  $\kappa$  and  $b_y$  in their respective positions, then the  $\varphi$  and  $\omega$  derived from the horizon camera are introduced on the left and right plate holders. The next step is to remove the remaining  $y$ -parallax with  $b_x$ . This procedure is repeated until the parallaxes effected by  $\kappa$ ,  $b_y$ , and  $b_x$  are removed. Normally, there would not be any residual  $y$ -parallaxes in the stereo model due to  $\varphi$  and  $\omega$ , and the elements derived from the horizon camera need not be corrected. However, if there were residual  $y$ -parallaxes present, they must be removed with either  $\varphi$  or  $\omega$ ; then the average for  $\varphi$  and  $\omega$  for each camera is introduced, similar to the procedure outlined for the B-8 plotter.

#### 4.3.3 — *Horizon Camera Data Combined with Statoscope and Doppler Data*

When, in addition to the horizon camera, statoscope data is available, then the general  $\Phi$  or the  $b_x$  component can be computed from this data and introduced directly into the plotter. Our experience showed that the determination of general  $\Phi$  or  $b_x$ , using the procedure described in paragraphs 4.3.1 and 4.3.2, is more accurate than the  $b_x$  indicated by the statoscope.

However, the statoscope data combined with the data derived from the horizon photos and the Doppler navigator make possible a method of bridging which permits the plotting of any model within a strip, without the necessity of triangulating all stereo models in the strip. Fig. 14 shows

the principle of this method. Assuming that in one stereo model of a strip, the flying height above a vertical datum can be determined, then, using the statorscope data, it is possible to compute the flying height above the same vertical datum for each vertical aerial photograph of the same strip. We know then the following elements of absolute orientation for each stereo model within each strip :

- (1) tip and tilt determined from the horizon camera
- (2) flying height relative to a vertical datum
- (3) the base distance between each exposure given by Doppler data, and consequently the scale.

The slope of the barometric surface can be determined either from formula (3), or by having a known ground elevation at the end of the flight line and comparing the computed flying height with the one determined from the ground control (Fig. 14).

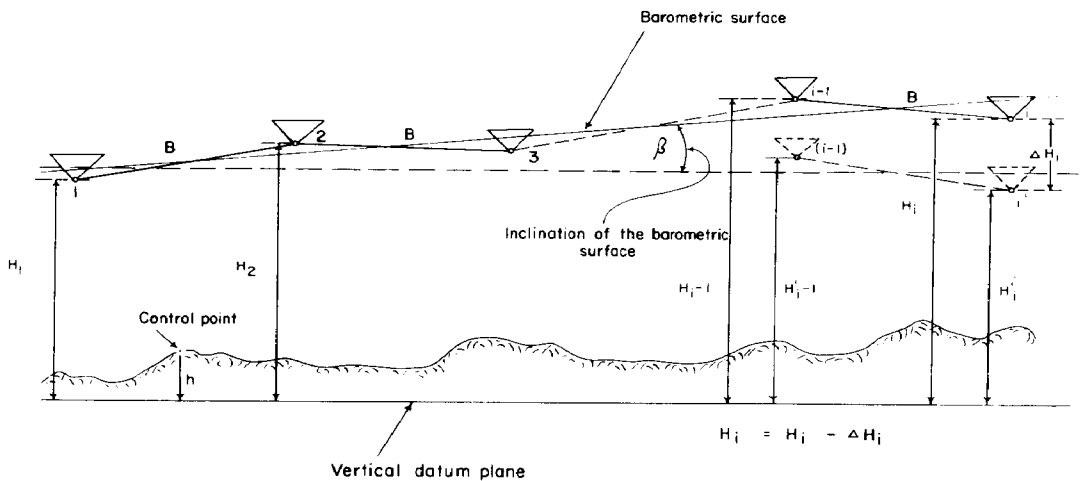


FIG. 14

The above information permits plotting any model within a strip at a correct scale and a correct vertical datum without the necessity of bridging the entire strip in a stereo-plotting instrument. Independent stereo models of many strips can be combined into one block which can then be adjusted.

It can easily be seen that the accuracy of transferring the vertical datum from the camera stations to the terrain by the above method depends largely on the accuracy of the base distance (scale), or the accurate knowledge of the terrain clearance. The accurate scale can be determined either from a horizontal block adjustment prior to the vertical adjustment, or directly from an Airborne Profile Recorder, provided the terrain is not covered with heavy vegetation and is relatively flat.

## 5. — ADJUSTMENT OF AERIAL TRIANGULATION

The adjustment of strips when auxiliary data is introduced in the aerial triangulation procedure must be approached differently from that of



the aero-polygon method. When the latter method is used, the adjusting procedure revolves around elimination of large errors in elevation caused by a double summation of accidental and systematic errors, and also by the influence of the earth's curvature. This is usually accomplished by means of second- and third-order functions. The variations from this ideal function of errors are not taken into account, although they undoubtedly exist.

When auxiliary data is utilized, the absolute orientation in space of each stereo model is independent of other stereo models; consequently the propagation of errors is quite different and generally follows a linear function (Fig. 15). The double summation of errors does not take place; therefore vertical control in the center of a strip has no real value. The closing errors before adjustment are considerably smaller than when the aero-polygon method is employed. However, there are, within a strip, undulations or local irregularities caused by inaccuracies in the auxiliary data and in the relative orientation. These are considered in the adjusting procedure if they are of a significant magnitude.

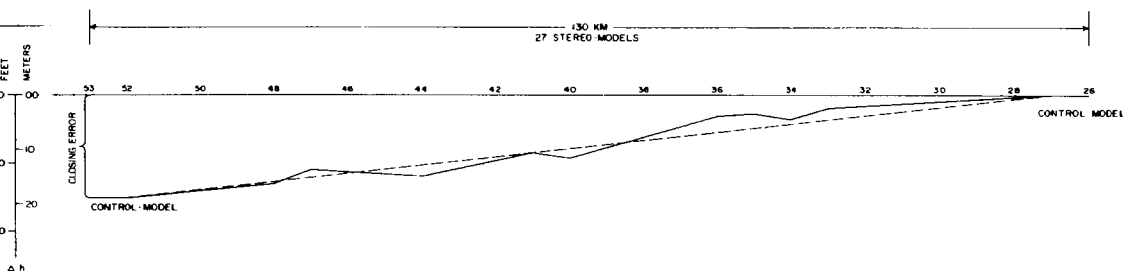


FIG. 15. — Actual errors in elevation observed in the center of strip #5 bridged using horizon photographs and Doppler data. Dashed line shows linear adjustment.

The first step in the adjustment is to bring all independent stereo models to a common vertical datum. Here, the independent stereo models can be formed into strips coinciding with the flight lines, or into strips across flight lines formed of stereo models from adjacent flight lines, or into blocks.

In our work in Nigeria and in Canada we combined independent stereo models of the same flight line into one strip and then combined the strips into one block. This is done mathematically by applying a vertical translation, so that the elevation of the center pass point in model  $n + 1$  agrees with the elevation of the same pass point in model  $n$ . The discrepancies between models due to  $\omega$  influence are adjusted individually and then the closing error in the elevation, observed in the last stereo model of the strip (ground control model), is distributed linearly. Presently, we are investigating procedures for simultaneous adjustment of independent stereo models with electronic computers.

The vertical block adjustment would be a relatively simple operation if it could be assumed that each strip is free from the influence of residual errors in  $\omega$ . In this case, the discrepancies in elevations on the common pass points between the adjacent strips could be adjusted by fitting to an average datum. However, there is always some  $\omega$  influence left in each strip.

The information at our disposal for the strip and block adjustment is :

1. closing error in elevation in the last stereo model of the strip,
2. the difference in  $\varphi$  and  $\omega$  determined for the common photographs from two adjacent models, for photograph  $i$ , from model  $(i-1, i)$  and model  $(i, i+1)$ ,
3. the differences in elevation on common pass points between adjacent strips,
4. the reliability of auxiliary data, and
5. the general "behaviour" of the strip during aerial triangulation.

The discrepancies in elevation observed at the common pass points between adjacent strips are mainly due to the following causes :

1. residual errors in  $\omega$  direction,
  2. residual undulations of the strip in the  $\varphi$  direction or "datum" differences,
  3. errors in stereoscopic reading of the elevations of the pass points,
  4. errors due to transferring of pass points between flight lines.
- Separation of these different errors is extremely difficult, if not impossible.

The block adjustment was done graphically. This permitted a quick evaluation of differences between strips. A "cross-section profile" of the block, perpendicular to the direction of the strips, was plotted in terms of elevation differences between adjusted strips.

The "profiles" were plotted at intervals equivalent to the location of common pass points. These "profiles" are then interpreted and an appropriate adjustment is made. For example, a profile, as shown on Fig. 16, indicates that strip No. 2 is "out of datum". The proper adjustment will be as indicated by the dashed line. A profile, as shown on Fig. 17, indicates that line 2 has an  $\omega$  error. The proper adjustment is indicated by the dashed line.

## 6. — EXTENSION OF HORIZONTAL CONTROL

On the projects in Nigeria, Gabon, and Canada, the horizontal control was extended by employing the well-known stereo-template method. The stereo templates were prepared at the same time as the vertical bridging. Presently, we are experimenting with an analytical method of adjustment of independent stereo models in a block. The method of "A Simultaneous Section Adjustment for Small Computers", by J. J. THERRIEN, and the method of "Three-Dimensional Transformation of Higher Degrees", by E. M. MIKHAIL, appear to be the most promising for this purpose.

## 7. — ACCURACY OF THE MAPPING SYSTEM

The mapping system described in the previous paragraphs was successfully employed in Africa and Canada. On these projects almost

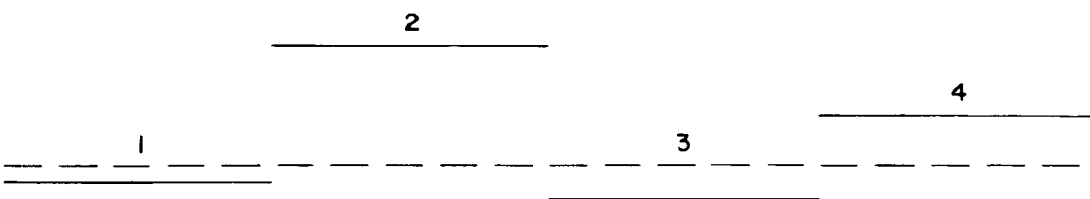


FIG. 16

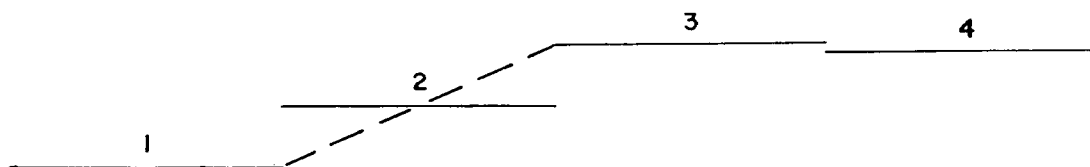


FIG. 17

5 000 vertical aerial photographs were triangulated. The experience gained on these projects permits an evaluation of its economy and accuracy under widely diverse atmospheric and climatic conditions.

### 7.1 — Experience in Nigeria

To determine the accuracy of this method under the operating conditions likely to be encountered in the broad project, a test area was established in Nigeria in the fall of 1961. This test area measured approximately  $34 \times 34$  miles ( $55 \times 55$  km). It was covered by nine flight lines of photography averaging 15 stereo models each. Ground control was established at both ends of each line. In addition, 97 vertical points were established throughout the test area to provide a sound basis for the evaluation of the accuracy of the proposed aerial triangulation method. This vertical control was established by third-order levels and stadia to an accuracy of better than  $\pm 5$  feet ( $\pm 1.5$  metres).

#### 7.1.1 — Accuracy of $\varphi$ and $\omega$ Determined from Horizon Camera Data and the Accuracy of General $\Phi$ Determined from Statoscope Data

To evaluate the accuracy of the orientation elements, a number of stereo models was oriented absolutely in the B-8 using ground control. The orientation elements  $\varphi$  and  $\omega$  of the right and left plate holder were registered with the L-shaped bubbles. These elements were then compared with the  $\varphi$  and  $\omega$  determined from horizon pictures. Also, the general  $\Phi$  determined from the ground control set-ups was compared with the general  $\Phi$  determined from statoscope data.

The mean square errors of the absolute orientation elements  $\varphi$  and  $\omega$  determined from horizon camera data and of general  $\Phi$  from statoscope data are as follows :

$$\begin{aligned} m\varphi &= \pm 4^{\circ} \quad (\text{based on } 30 \text{ comparisons}) \\ m\omega &= \pm 6^{\circ} \quad (\text{based on } 32 \text{ comparisons}) \\ m\Phi &= \pm 7^{\circ} \quad (\text{based on } 19 \text{ comparisons}). \end{aligned}$$

The higher error in  $\omega$  is due to an instability of the B-8 in the  $\omega$  direction of about  $\pm 2^\circ$ .

### 7.1.2 — Accuracy of Aerial Triangulation

The test area is shown on Fig. 18. Strips were adjusted separately to vertical ground control established only at the beginning and at the end (i.e., at 15-model intervals) of each strip. The residual errors in elevation after block adjustment, based on 97 vertical control points spread throughout the test area, are as follows :

87 % within  $\pm 10$  feet ( $\pm 3.1$  metres)

92 % within  $\pm 12.5$  feet ( $\pm 3.9$  metres)

98 % within  $\pm 16.5$  feet ( $\pm 5.1$  metres)

Only two points showed errors greater than 16.5 feet (5.1 metres), one of 18 feet (5.6 metres), and one of 21 feet (6.5 metres). The mean square error in elevation is  $m_H = \pm 6.8$  feet, or approximately  $\pm 2$  metres.

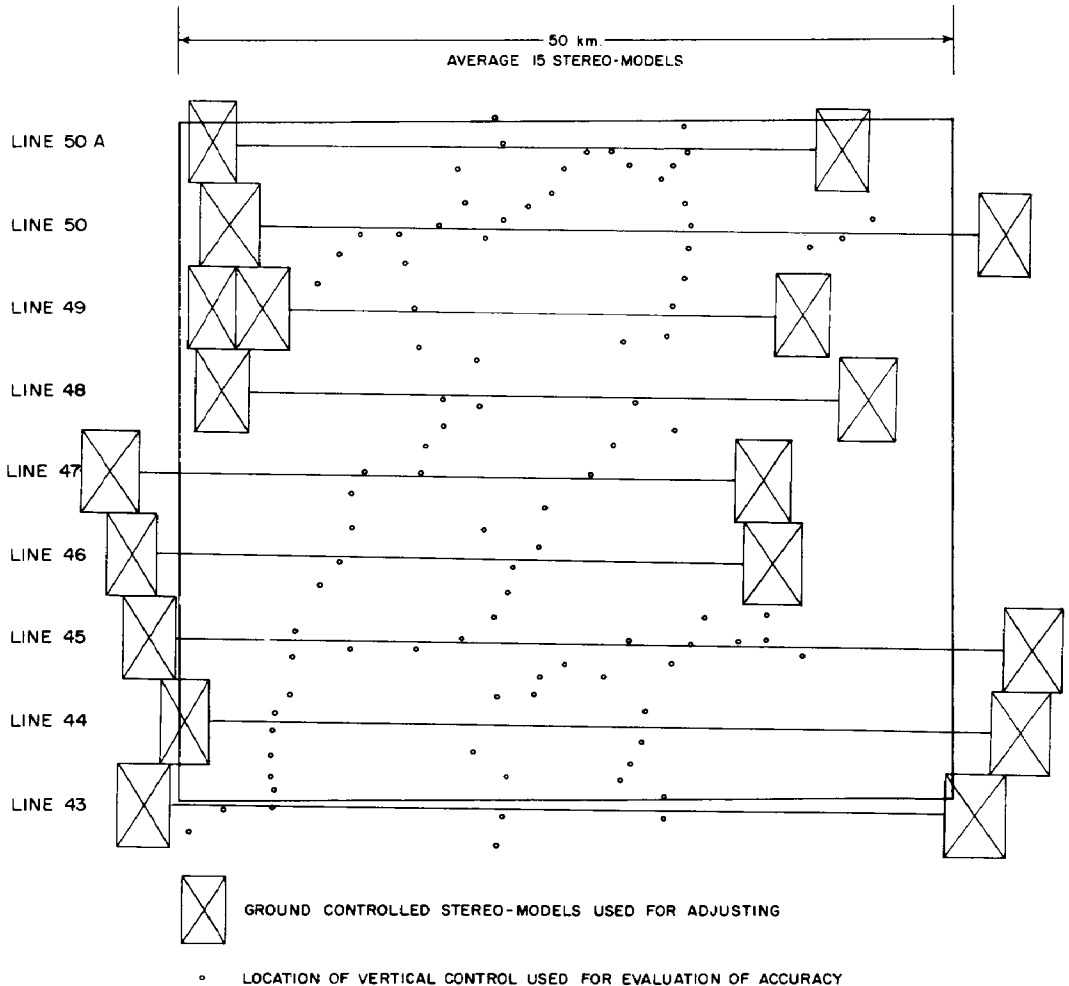


FIG. 18. — Test area in Nigeria.

7.2 — Results Obtained in Canada

The project area was located in the northern part of the province of Alberta, south of Lake Athabasca. It measured  $100 \times 40$  miles ( $160 \times 64$  km) and was covered with 8 flight lines consisting of 40 stereo models each. The aerial photography was flown with a Wild RC-9 camera at a scale of 1/50 000.

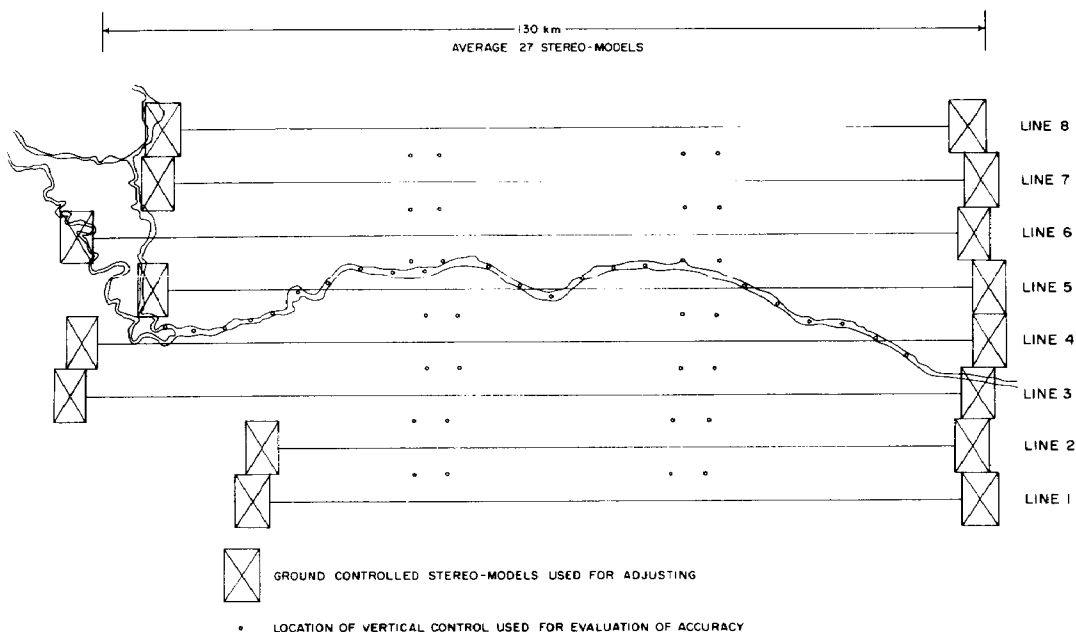


FIG. 19. — Portion of a project area in Canada where vertical control was available for evaluation of the accuracy of the mapping system.

7.2.1 — Accuracy of  $\varphi$  and  $\omega$  Determined from Horizon Camera

A total of 28 stereo models was oriented absolutely in the B-8 plotter using ground elevations or water bodies. The tip and tilt of the left and right photographs were read using the L-shaped bubbles, giving absolute values for  $\varphi$  and  $\omega$  for each picture. These values were then compared with the values of  $\varphi$  and  $\omega$  derived from horizon pictures. The results based on 56 comparisons are as follows :

$d\varphi$	%
$0^c \text{ --- } \pm 2^c$	77
$\pm 2^c \text{ --- } \pm 3^c$	11
$\pm 3^c \text{ --- } \pm 4^c$	5
$\pm 4^c \text{ --- } \pm 5^c$	7

$d\omega$	%
$0^c \text{ --- } \pm 2^c$	56
$\pm 2^c \text{ --- } \pm 3^c$	14
$\pm 3^c \text{ --- } \pm 4^c$	7
$\pm 4^c \text{ --- } \pm 7^c$	23

The mean square errors of  $\varphi$  and  $\omega$  are as follows :

$$m\varphi = \pm 2^c.2$$

$$m\omega = \pm 3^c.6$$



FIG. 20. — Aerial photograph taken in Nigeria with a Wild RC-9 camera equipped with super-infragon lens and using infra-red film.

The lower accuracy in  $\omega$  can be explained again by the fact that the B-8 has an instability in the  $\omega$  direction of approximately  $\pm 2^\circ$ , which influences the determination of the values for absolute  $\omega$  in the plotter.

In addition, we also evaluated the accuracy of tip and tilt determined by comparing horizon pictures of adjacent flight lines and using only one ground-controlled stereo model in the block. Horizon pictures of different flight lines flown on the same day were measured in the stereo microscope using a single reference picture for the entire block. For example, if Line 1 were flown north, and Line 2, south, then the forward horizon photographs of Line 1 would be compared with a reference aft horizon photograph of Line 2 for the determination of differential  $\varphi$ . We chose picture 52 of Line 3 as the reference picture and determined  $\varphi$  for the ground-controlled aerial photographs in Lines 1, 2, 4, 5, 7, and 8. The results are as follows :

**Determination of  $\varphi$**

	Line 1	Line 2	Line 3	Line 4	Line 5	Line 7	Line 8
			Reference				
Print No. ....	58	73	52	62	52	142	153
Time (*) .....	16 <sup>h</sup> 58 <sup>m</sup>	17 <sup>h</sup> 03 <sup>m</sup>	18 <sup>h</sup> 49 <sup>m</sup>	18 <sup>h</sup> 53 <sup>m</sup>	22 <sup>h</sup> 27 <sup>m</sup>	20 <sup>h</sup> 40 <sup>m</sup>	20 <sup>h</sup> 42 <sup>m</sup>
From Ground							
Control .....	99±16 <sup>c</sup>	100±30 <sup>c</sup>	98±78 <sup>c</sup>	99±86 <sup>c</sup>	99±60 <sup>c</sup>	99±69 <sup>c</sup>	99±77 <sup>c</sup>
From Horizon ....	99±15 <sup>c</sup>	100±31 <sup>c</sup>		99±81 <sup>c</sup>	99±55 <sup>c</sup>	99±69 <sup>c</sup>	99±80 <sup>c</sup>
Print No. ....			46				
Time (*) .....			18 <sup>h</sup> 40 <sup>m</sup>				
From Ground							
Control .....			100±41 <sup>c</sup>				
From Horizon ....			100±42 <sup>c</sup>				
	↑	↓	↑	↓	↑	↑	↑
Print No. ....			38	84	36		173
Time (*) .....			18 <sup>h</sup> 30 <sup>m</sup>	19 <sup>h</sup> 15 <sup>m</sup>	22 <sup>h</sup> 00 <sup>m</sup>		21 <sup>h</sup> 05 <sup>m</sup>
From Ground							
Control .....			100±85 <sup>c</sup>	99±73 <sup>c</sup>	100±90 <sup>c</sup>		100±04 <sup>c</sup>
From Horizon ....			100±86 <sup>c</sup>	99±70 <sup>c</sup>	100±85 <sup>c</sup>		100±03 <sup>c</sup>
		↓	↑	↓	↑		↑
Print No. ....			30	93			
Time (*) .....			18 <sup>h</sup> 20 <sup>m</sup>	19 <sup>h</sup> 25 <sup>m</sup>			
From Ground							
Control .....			99±83 <sup>c</sup>	100±57 <sup>c</sup>			
From Horizon ....			99±85 <sup>c</sup>	100±59 <sup>c</sup>			
Print No. ....	25	102	16	97	18	109	186
Time (*) .....	15 <sup>h</sup> 48 <sup>m</sup>	17 <sup>h</sup> 42 <sup>m</sup>	17 <sup>h</sup> 53 <sup>m</sup>	19 <sup>h</sup> 33 <sup>m</sup>	21 <sup>h</sup> 37 <sup>m</sup>	19 <sup>h</sup> 45 <sup>m</sup>	21 <sup>h</sup> 26 <sup>m</sup>
From Ground							
Control .....	98±91 <sup>c</sup>	100±45 <sup>c</sup>	100±30 <sup>c</sup>	99±86 <sup>c</sup>	99±81 <sup>c</sup>	100±88 <sup>c</sup>	99±97 <sup>c</sup>
From Horizon ....	98±95 <sup>c</sup>	100±44 <sup>c</sup>	100±28 <sup>c</sup>	99±81 <sup>c</sup>	99±76 <sup>c</sup>	100±87 <sup>c</sup>	99±97 <sup>c</sup>

For the determination of  $\omega$  chose picture 62 of Line 4 as the reference. The results are as follows :

**Determination of  $\omega$**

	Line 1	Line 2	Line 3	Line 4	Line 5	Line 7	Line 8
				Reference			
Print No. ....	57	73	52	62	53	145	154
Time (*) .....	16 <sup>h</sup> 56 <sup>m</sup>	17 <sup>h</sup> 03 <sup>m</sup>	18 <sup>h</sup> 49 <sup>m</sup>	18 <sup>h</sup> 53 <sup>m</sup>	22 <sup>h</sup> 29 <sup>m</sup>	20 <sup>h</sup> 41 <sup>m</sup>	20 <sup>h</sup> 43 <sup>m</sup>
From Ground							
Control .....	100±18 <sup>c</sup>	100±15 <sup>c</sup>	98±95 <sup>c</sup>	101±00 <sup>c</sup>	100±15 <sup>c</sup>	99±17 <sup>c</sup>	100±07 <sup>c</sup>
From Horizon ....	100±14 <sup>c</sup>	100±12 <sup>c</sup>	98±92 <sup>c</sup>		100±18 <sup>c</sup>	99±18 <sup>c</sup>	100±06 <sup>c</sup>
	↑	↓	↑	↓	↑	↑	↑

(\*) Time shown is Greenwich time.

The arrows indicate the direction of flight. Note that the elapsed time between the exposure of the reference picture and the exposure of the measured pictures is as much as 3<sup>h</sup>38<sup>m</sup> and yet this time difference did not affect the accuracy of the determination of  $\varphi$ . The accuracy, both in  $\varphi$  and  $\omega$ , is remarkably high. The maximum difference between the  $\varphi$  and  $\omega$  determined in this way from horizon pictures and the values of  $\varphi$  and  $\omega$  determined from absolute orientation on ground control is only 5°. The mean square errors are :

$$m\varphi = \pm 2^{\circ} \quad (\text{based on 20 comparisons})$$

$$m\omega = \pm 2^{\circ} \quad (\text{based on 6 comparisons}).$$

### 7.2.2 — Accuracy of General $\Phi$ Derived from Statoscope and Horizon Camera Data

The inclination of the base was determined from the statoscope data, as well as by the procedure described in section 4.3.1 for utilizing the horizon camera data. The comparison of these values with the general  $\Phi$  determined from absolute orientation of the stereo models from ground control gives the following standard errors of general  $\Phi$  :

- (a) determined from statoscope .....  $m\Phi = \pm 5^{\circ}$   
 (b) determined from horizon camera .....  $m\Phi = \pm 2.8^{\circ}$

Using the average base distance for the photography of the project, the above values are equivalent to an error in elevation of  $\pm 12.5$  feet ( $\pm 3.9$  metres) and  $\pm 7$  feet ( $\pm 2.2$  metres) respectively. The above results demonstrate that the horizon camera provided more accurate results than the statoscope.

### 7.2.3 — Accuracy of Aerial Triangulation

To evaluate the accuracy of aerial triangulation over long distances using the horizon camera data, a block of 8 strips was chosen. Each strip was 130 km long and comprised an average of 27 stereo models. The photography was flown with a Wild RC-9 camera at 1/50 000. Fig. 15 illustrates the actual errors in elevation observed in Strip 5 before any adjustment was made. They are typical of strips bridged using horizon data. From this figure it can be seen that errors in elevation propagate linearly. After bridging a length of 130 km (27 stereo models), the closing error is only 61 feet (19 metres). The closing errors in other strips were of the same order of magnitude.

Adjustment of all eight strips and of the block was carried out utilizing vertical control only at the beginning and at the end of each strip. A sketch of the area showing the layout of the flight lines and location of ground control is shown on Fig. 19.

To determine the residual errors in elevation after block adjustment, known elevations of 50 points located within the block were compared with the elevations established photogrammetrically. The results are :

$\Delta h$ in feet	$\Delta h$ in metres	%
0 — $\pm 5$	0 — $\pm 1.5$	50
$\pm 5$ — $\pm 10$	$\pm 1.5$ — $\pm 3.1$	30
$\pm 10$ — $\pm 15$	$\pm 3.1$ — $\pm 4.6$	10
$\pm 15$ — $\pm 20$	$\pm 4.6$ — $\pm 6.2$	10



The mean square error in elevation observed on these points is  $m_H = \pm 9$  feet, or approximately  $\pm 3$  metres.

### 7.3 — Accuracy of Doppler Distance Measurements

To evaluate the accuracy of the scale determined from Doppler navigator data, we compared the base distance given by Doppler with the base distance derived from scaling of stereo models to the positions obtained from stereo-template laydown. The results obtained, both in Nigeria and in Canada, show that the mean square error, relative to the base distance, is  $\pm .27\%$ , or  $\pm 1/370$ .

## 8. — CONCLUSIONS

The instruments and methods described in this paper were employed in Nigeria, Gabon, and Canada on practical mapping projects covering some 115 000 km<sup>2</sup>, so the results achieved are indicative of the accuracies that can be expected from this mapping system under diverse operational conditions. The results of these surveys support the following conclusions :

- (1) The horizon camera permits determination of the tip and tilt of the aerial camera at the moment of exposure with the same order of accuracy as the accuracy of relative and absolute orientations of a stereo model based on ground control.
- (2) The horizon camera data permits an accurate determination of the nadir point needed in connection with Aerodist- or Hiran-controlled photography.
- (3) The aerial triangulation can be carried out on a simple and relatively inexpensive instrument, such as a Wild B-8 plotter.
- (4) Since the bridging is done with independent pairs, a number of plotting instruments can be used simultaneously for bridging of the same strip.
- (5) The mapping system is independent of the terrain (unlike the A.P.R. system).
- (6) The density of the vertical control when mapping a large area is reduced by as much as 50 %, compared with the aero-polygon method.
- (7) Because there is no rigid requirement regarding the location of the ground control within a strip, such control can be established at locations where the access is best and where good photo identification can be accomplished.
- (8) The application of this mapping system makes a new approach to aerial triangulation feasible. It is no longer necessary to bridge in strips. Independent stereo models can be combined immediately into blocks and adjusted. Bridging of blocks can now be directly done, instead of first bridging strips.

- (9) The accuracies achieved indicate that the horizon camera could provide useful data for large scale mapping.
- (10) The vertical accuracy of elevations established in aerial triangulation is not materially influenced by the length of the strip.
- (11) The capital acquisition costs of the horizon camera and statorscope are relatively modest, and the equipment can be installed in a small aircraft.
- (12) The operation of the equipment is simple, and the instruments are very reliable and virtually free from breakdowns.

### BIBLIOGRAPHY

- [1] GRUBER, O.V. : Horizontbilder und ihre Verwendung, *Phot'ia* 1940, pp. 61-70.
- [2] HELAVA, U.V. : Horizon Camera Method, *The Canadian Surveyor*, XIII, 8, 1957.
- [3] LÖFSTRÖM, K. G. : Horizontkontrollierte Aeropolygonierung, Publ. No. 46, Finn. Geod. Inst. 1955.
- [4] MIKHAIL, E. M. : Simultaneous Three-Dimensional Transformation of Higher Degrees, *Photogr. Eng.*, July 1964.
- [5] SCHERMERHORN, W. : History and Development of Aerial Triangulation, *Rivista dell'Istituto Geografico Militare*, Ottobre 1960 (Numero Speciale).
- [6] THERRIEN, J. J. : A Simultaneous Section Adjustment for Small Computers, *The Canadian Surveyor*, December 1963.
- [7] ZARZYCKI, J. M. : Super-Infragon Photography and Auxiliary Data on a Mapping Program for Nigeria, *The Canadian Surveyor*, March 1963.
- [8] ZARZYCKI, J. M. : New Aerial Triangulation Techniques Employed on a Mapping Project in Nigeria, *Photogrammetric Engineering*, July 1963.